

# Conformational Free Energy of Lattice Polyelectrolytes with Fixed Endpoints. I. Single-Chain Simulation and Theory

Th. M. A. O. M. Barenbrug,\* J. A. M. Smit, and D. Bedeaux

Gorlaeus Laboratories, Leiden Institute of Chemistry, University of Leiden, P.O. Box 9502, 2300 RA Leiden, The Netherlands

Received July 5, 1996; Revised Manuscript Received October 7, 1996<sup>®</sup>

**ABSTRACT:** Using Monte Carlo methods, the conformational free energy of an isolated lattice polyelectrolyte with fixed endpoints was calculated directly as a function of the chain length, the number of charges on the chain, the end-to-end distance of the chain, and the value of the Debye screening length. Lattice polyelectrolytes are self-avoiding random walks on a cubic lattice, bearing equidistantly-fixed, discrete charges. For the electrostatic interaction, a Debye–Hückel potential is used. To comprehend the simulation data, a descriptive analytical expression is proposed, which gives, in particular for charge densities around Manning's condensation threshold, a good estimate for the conformational free energy of a polyelectrolyte chain as a function of the relevant parameters. Furthermore, the simulation data are compared to the predictions of the theory of Katchalsky for a Gaussian chain with fixed endpoints and with screened electrostatic interactions between the charged segments. The derivation of this expression and the approximations involved are reinspected, and a better expression for the description of this model is proposed. For charge densities below Manning's condensation threshold, the results of this expression are in good agreement with the simulation data.

## 1. Introduction

Due to their capability of absorbing very large amounts of water and dilute solutions, polyelectrolyte networks are often referred to as “hydrogels”. In various compositions, these substances have found a wide range of applications in chemistry, medicine, agriculture, and personal care. In spite of this broad practical interest, a completely satisfactory theoretical description of the swelling behavior of polyelectrolyte gels is not yet available.

Most theories developed until now have a lot of features in common. The chains that constitute the swollen network usually are supposed to be more or less stretched between the cross-links, which connect (by definition) the endpoints of several of these chains. Although the positions of the cross-links will show fluctuations around their equilibrium, in a first approximation one assumes that, in a swollen gel in equilibrium, these positions are more or less fixed, as the strong elastic forces that are present allow only small fluctuations around these positions.

In most theories, the interactions between (charged) segments of different chains in the network are neglected, so that the chains are effectively treated as independent, except for the positions of their endpoints. This simplification is allowed when a sufficient amount of added salt is present, assuring a relatively small Debye screening length, and at the same time the gel is sufficiently swollen so that all interactions between segments of different chains can be neglected.

Starting from the above assumptions, the total free energy of the gel is obtained by adding three contributions: the electrostatic and elastic free energy of the chains between the fixed cross-links, the free energy associated with the mixing process of polymer and solution, and the free energy of the salt ions, unequally distributed between the internal solution and the surrounding medium (the “Donnan effect”). The expressions for the latter two contributions can easily be

given,<sup>1</sup> if one supposes that swelling of the gel occurs in an affine manner. This will be more or less the case if the polymer and cross-linking agent are homogeneously distributed in the gel. Other contributions to the free energy (e.g., kinetic contributions) are not considered.

Clearly, the conformational free energy of the charged chains that constitute the network plays a central role. Many studies have been undertaken that somehow assemble this quantity from the average electrostatic free energy of a Gaussian chain molecule with a fixed end-to-end distance and an entropy which is strictly related to the conformations of the equivalent uncharged chain.<sup>2–4</sup> Some authors describe very weakly charged gels and do not account for the electrostatic interactions between segments at all,<sup>5,6</sup> while others overestimate these effects, by assuming that effectively the chains are completely stiff rods.<sup>7</sup>

Theoretical calculations of the conformational free energy which incorporate the electrostatic interactions usually overestimate the actual swelling behavior found in highly charged gels. This is because the charged chains are assumed to be Gaussian and thus very flexible, allowing their segments to approach each other as frequently as in the uncharged case, so that the averaging process results in a strong overestimation of the charge interactions between segments located relatively far away from each other on the chain's backbone. Besides, the polyelectrolyte chains that form a charged network are usually relatively short and, in the swollen state, also rather stiff and stretched. Therefore, the question arises whether the concept of Gaussian chains leads to a realistic model.

A straightforward pathway to investigate this point would be the Monte Carlo determination of the conformation integral—and, consequently, the conformational free energy—of a partially charged chain of segments (beads) and bonds (sticks) with a fixed end-to-end distance, a fixed angle between neighboring bonds, and hindered rotation around the bonds to mimic the rotational behavior of the C–C bonds in the backbone of the polyelectrolyte molecule. This kind of simulations

<sup>®</sup> Abstract published in *Advance ACS Abstracts*, January 15, 1997.

is, however, difficult to perform because of the constraint of the fixed end-to-end distance.

In an earlier paper,<sup>8</sup> we described lattice polyelectrolytes with free endpoints. We found that their average properties match quite well the results of the much more detailed chain models consisting of bead-and-stick chains with fixed bond angles and hindered rotation in continuous space. We also found that the effect of charge mobility (which occurs in the case of weak polyelectrolytes) is relatively small. Therefore, we employ the same lattice chain model as before to calculate the conformational free energy of polyelectrolyte chains, but now with their endpoints and charges fixed. A brief description of the model and calculation methods used is given in section 2. The third section briefly presents the results obtained for chains of 10, 20, 40, and 80 segments, for four different values of the Debye screening length, for different charge densities and various fixed end-to-end distances. In section 4, we discuss our findings regarding the behavior of the conformational free energy of charged lattice chains with fixed endpoints. An analytical approximation for this conformational free energy is proposed, and in section 5, the results are compared to predictions following from the theory of Katchalsky. This theory is improved to incorporate the influence of charge interactions on the segment distribution of a charged Gaussian chain, and the results are discussed. In section 6, we present our conclusions.

## 2. Model and Methods

The model polyelectrolyte consisting of  $n + 1$  segments, and thus linked by  $n$  bonds, is represented by an  $n$ -step self-avoiding random walk (SAW) on a (three-dimensional) cubic lattice.  $q$  of the segments are charged with the elementary charge  $e$ . As in our earlier work,<sup>8</sup> the segments are given a length of  $a = 2.515 \times 10^{-10}$  m, which is appropriate for acrylic acid. In the following, all distances are expressed in terms of this unit length. Every polyion conformation is represented by  $\{\mathbf{r}_i, Q_i\}$ , where  $\mathbf{r}_i$  ( $i \in \{0, 1, \dots, n\}$ ) describes the position of the  $i$ th segment and  $Q_i$  is either 0 or 1, depending on whether the  $i$ th segment is charged or not. The  $q$  charges are positioned equidistantly (as far as is possible on the discrete lattice), and their number and positions along the chain, as well as the positions of the first and last segment, are kept fixed during the Monte Carlo simulation. In previous work,<sup>8</sup> we studied the influence of charge mobility on the equilibrium properties of lattice polyelectrolytes. As one might expect, mobility of the charges, which occurs in partially neutralized weak polyelectrolytes, leads effectively to a redistribution of charge on the polyelectrolyte backbone, resulting in an effective shift of the charges toward both chain ends. As a result, the middle part of the chain is less charged, so more compact conformations of that part of the chain can be attained. In this way, the chain's radius of gyration is reduced, and its entropy is favored. Relative changes in the expansion of the chains of at most 10% were found in this way. The introduction of charge mobility in a polyelectrolyte network will, however, result in smaller changes in the chain's behavior, as an effective redistribution of the charges toward the chain ends (*i.e.*, toward the cross-links) will be counteracted by the electrostatic repulsion of the charges of neighbor chains connected to this same cross-link. It is, therefore, to be expected that charge mobility will introduce only slight modifications and thus only minor changes in the polyelectrolyte behavior. We did not investigate this point any further for the present problem.

The charges are assumed to interact according to a Debye-Hückel potential, which is given as a function of the distance  $r$  by

$$\psi(r) = \frac{ee^{-\kappa r}}{4\pi\epsilon r} \quad \text{where} \quad \kappa^2 = \frac{1000N_A e^2 C_0}{\epsilon kT} \quad (2.1)$$

in which  $\kappa$  is the reciprocal Debye screening length,  $N_A$  is the Avogadro number,  $e$  is the elementary charge,  $C_0$  is the concentration of small ions present (in mol/L),  $\epsilon$  is the dielectric constant of the solvent,  $k$  is the Boltzmann constant, and  $T$  is the absolute temperature (all quantities in SI units). The Debye-Hückel potential is most appropriate if the system contains only monovalent small ions.<sup>9</sup> The use of this potential makes the model particularly appropriate for weak polyelectrolytes.<sup>10</sup> In real systems, the phenomenon of counterion condensation<sup>11</sup> should be taken into account for charge densities higher than about 35% (estimated for a line charge, with the chosen value of  $a = 2.515$  Å), which results, for theoretical charge densities higher than this threshold value, in an effective lowering of the charge density to this value. The reason for considering also larger charge densities in this paper is to make our treatment comparable with other theories that do not take condensation effects into account.

The usual statistical mechanical approach implies that every average property  $\langle A \rangle$  of the system (which must depend on positional parameters only) can be computed by averaging its value over all conformations of the system, using the Boltzmann factor of every conformation as the weight factor for that particular conformation:

$$\langle A \rangle \equiv \sum_c p_c A_c \quad (2.2)$$

Here,  $c$  counts all possible conformations. The probability of the conformation  $c$ , which has the energy  $E_c$ , is given by

$$p_c = \frac{e^{-\beta E_c}}{\sum_c e^{-\beta E_c}} = \frac{e^{-\beta E_c}}{Z} \quad (2.3)$$

where  $Z$  represents the partition sum and  $\beta$  has its usual meaning of  $1/kT$ . In the canonical ensemble, the entropy is given by the average

$$S = -k\langle \ln(p_c) \rangle = -k \sum_c p_c \ln(p_c) \quad (2.4)$$

Substituting eq 2.3 into 2.4 leads to

$$S = +k \ln(Z) + \beta k \sum_c p_c E_c = k \ln(Z) + \frac{\langle E \rangle}{T} \quad (2.5)$$

By means of eq 2.5 and the thermodynamic expression  $F = U - TS = \langle E \rangle - TS$ , one obtains for the conformational free energy of the system the well-known equation

$$\beta F = -\ln(Z) \quad (2.6)$$

Note that kinetic contributions are not included in this treatment. They appear as additional terms. As, generally, all average properties of interest in this study involve derivatives of the free energy with respect to *positional* parameters, the kinetic terms do not contribute and are, therefore, omitted directly.

To obtain the conformational free energy of the lattice polyelectrolytes studied here, we need an expression for  $Z$ . Usually this quantity requires a summation over *all* possible conformations of the self-avoiding walk for every value of  $R$ . This calculation would be far too time-consuming. Rather, one would employ some average quantity, to be obtained by sampling (for every value of  $R$ ) only a relatively small (but sufficiently representative) part of conformation space. For that purpose, we introduce the quantity

$$\langle e^{+\beta E} \rangle \equiv \frac{\sum_c e^{+\beta E_c} e^{-\beta E_c}}{\sum_c e^{-\beta E_c}} = \frac{c_n(R)}{Z} \quad (2.7)$$

where  $c_n(R)$  is the total number of possible conformations of

the self-avoiding walk of  $n$  steps, its endpoints being fixed at a distance  $R$ . The value of  $c_n(R)$  can be estimated by first calculating the exact number of different  $n$ -step ordinary random walks between the two fixed endpoints (see Appendix 1) and subsequently determining the fraction of them that is also self-avoiding, using simple sampling techniques.

From eqs 2.6 and 2.7, we find

$$\beta F = -\ln\left(\frac{c_n(R)}{\langle e^{+\beta E} \rangle}\right) = -\ln(c_n(R)) + \ln(\langle e^{+\beta E} \rangle) \equiv \beta F_0 + \beta F_q \quad (2.8)$$

where  $\beta F_0$  and  $\beta F_q$  are the entropy of the uncharged chain and the electrostatic contribution to the free energy, respectively. Note that, for zero charge, the electrostatic contribution  $\beta F_q$  reduces to zero.

In the averaging process, we constructed random self-avoiding walks with fixed endpoints by means of a pivot algorithm, devised by Madras and Sokal.<sup>12</sup> This algorithm is similar to the one previously<sup>8</sup> used for free SAWs.<sup>13</sup> All conformations generated were used in the averaging process. Usually, averaging is performed in the way Metropolis proposed, by calculating the Boltzmann factor of every conformation and using this weight factor to decide whether the conformation under consideration should be included in the averaging process or not. In this way, low-energy conformations are favoured, as these supposedly give the most substantial contributions to the average. However, the quantity  $\exp(+\beta E)$  grows exponentially with the energy of the conformation, so that all attainable conformations contribute equally to the average (see eq 2.7). The bias on conformations of low energy introduced by the Metropolis algorithm therefore results in an underestimation of the value of  $\langle \exp(+\beta E) \rangle$ , as we could verify for chains of 10 segments by means of a computer program, in which the exact values were compared to the results of both averaging methods.

The (total) energy,  $E_c$ , of a particular polyon conformation  $c (= \{\mathbf{r}_i, Q_i\})$  is calculated by taking the sum over all screened pair interactions of the polyon charges,

$$\beta E = \sum_{i=0}^{n-1} \sum_{j=i+1}^n Q_i Q_j \frac{Q_i Q_j}{|\mathbf{r}_i - \mathbf{r}_j|} \exp(-\kappa |\mathbf{r}_i - \mathbf{r}_j|) \quad (2.9)$$

where  $Q (= e^2/4\pi\epsilon kT = 2.783a)$  is the Bjerrum length at room temperature. Equation 2.9 is used in computing average quantities, as described near eqs 2.2 and 2.3. Using the described algorithm, we could reproduce exact enumeration results for  $n \leq 10$  within a very small relative error ( $<0.1\%$ ), which indicated its correctness. Averaging for larger values of  $n$  was performed until the estimated relative error in the results was smaller than 5% for all chain lengths studied.

### 3. Results

In Tables 4–7 in Appendix 2, the results for the conformational free energy of lattice polyelectrolytes with fixed end-to-end distance  $R$  are presented for 11 different fractions of charged segments (0%, 10%, 20%, ..., 100%), for four different chain lengths ( $n = 9, 19, 39$ , and 79), and for four different values of the normalized inverse Debye screening length ( $\kappa a = 0.0, 0.3, 0.6, 0.9$ ). The value  $\kappa a = 0$  is included to enable interpolation of the results for small values of  $\kappa a$ . In the tables and graphs (but *not* in the equations) presented, the free energies are given in units  $kT$ , the total charge is expressed as the number of elementary charges, and the fixed end-to-end distance  $R$  is normalized with respect to the bond length  $a$ . Note that the maximum end-to-end distance of a chain of  $n + 1$  segments is  $R_{\max} = na$ . The absolute temperature  $T = 298$  K. For the longest chains ( $n = 79$  steps) there are no data available for  $R$  values below  $0.5na$ , as these calculations were very time consuming.

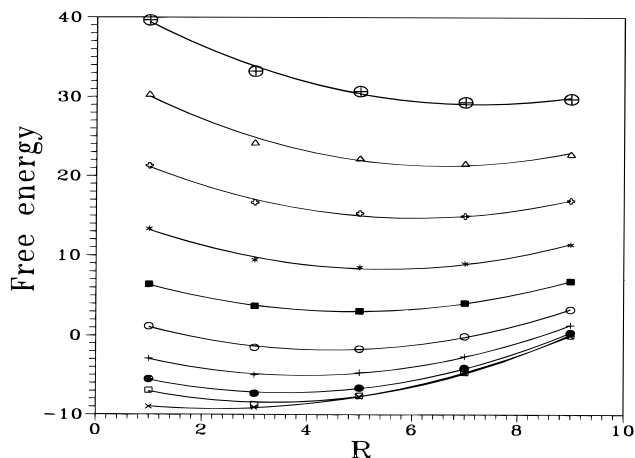


**Figure 1.** Conformational free energy (normalized by  $kT$ ) of a chain of 10 segments versus the fixed end-to-end distance  $R$  (normalized by  $a$ ), for a total of (bottom to top) 0 ( $\times$ ), 2 ( $\square$ ), 3 ( $\bullet$ ), 4 ( $+$ ), 5 ( $\circ$ ), 6 ( $\blacksquare$ ), 7 ( $*$ ), 8 ( $\star$ ), 9 ( $\Delta$ ), and 10 ( $\oplus$ ) elementary charges.  $\kappa a = 0.3$ .

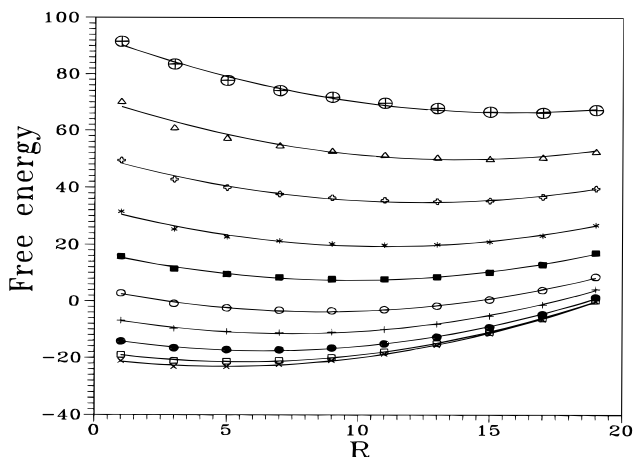


**Figure 2.** Conformational free energy (normalized by  $kT$ ) of a chain of 20 segments versus the fixed end-to-end distance  $R$  (normalized by  $a$ ), for a total of (bottom to top) 2 ( $\times$ ), 4 ( $\square$ ), 6 ( $\bullet$ ), 8 ( $+$ ), 10 ( $\circ$ ), 12 ( $\blacksquare$ ), 14 ( $*$ ), 16 ( $\star$ ), 18 ( $\Delta$ ), and 20 ( $\oplus$ ) elementary charges.  $\kappa a = 0.3$ .

### 4. Discussion

For the discussion of the results, eq 2.8 is helpful. In the case of zero charge, the interaction energy  $E_c$  is identical to zero. Equation 2.8 then leads to

$$\beta F = -\ln[c_n(R)] = \beta F_0 \quad (4.1)$$

Thus, the conformational free energy of the uncharged chain contains an entropy term only, *i.e.*,  $F = -TS$ . The entropy contains the number of possible conformations and is given by the well-known expression  $S = -k \ln(c_n(R))$ . Obviously, the number of conformations increases with decreasing value of  $R$ , *i.e.*, if the chain contracts. For the uncharged case, therefore,  $F$  increases monotonously with increasing  $R$  (see the lowest curve, for  $q = 0$ , in Figure 1).

In the limit of complete extension, *i.e.*,  $R = na$ , the chain can assume only one conformation ( $c_n(R) = 1$ ), and consequently  $F$  is identical to zero, *i.e.*,  $F(q = 0, R = na) = 0$ . Clearly, the same applies for  $n = 20$  and  $n = 40$  (in Figures 2 and 3, the curves for  $q = 0$  are not explicitly shown; they coincide for the larger part with the curves for  $q = 2$  and  $q = 4$ , respectively).

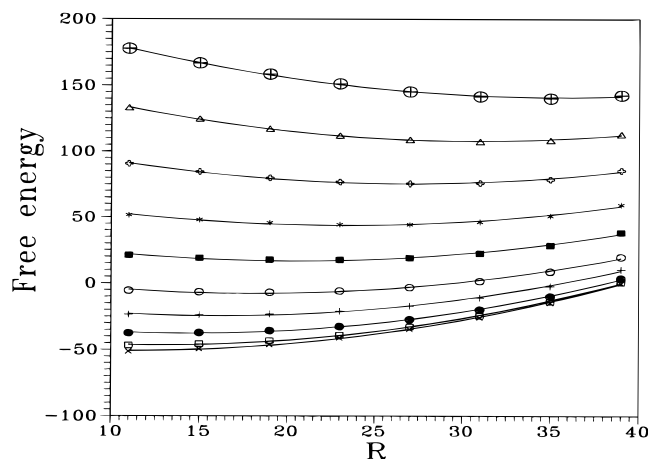


**Figure 3.** Conformational free energy (normalized by  $kT$ ) of a chain of 40 segments versus the fixed end-to-end distance  $R$  (normalized by  $a$ ), for a total of (top to bottom) 4 ( $\times$ ), 8 ( $\square$ ), 12 ( $\bullet$ ), 16 ( $+$ ), 20 ( $\circ$ ), 24 ( $\blacksquare$ ), 28 ( $*$ ), 32 ( $\star$ ), 36 ( $\triangle$ ), and 40 ( $\oplus$ ) elementary charges.  $\kappa a = 0.3$ .

For a completely stretched ( $c_n(R) = 1$ ) and charged chain, we find, using eq 2.8, that

$$\beta F = \ln\langle \exp(+\beta E) \rangle = \beta F_q \quad (4.2)$$

The interaction energy increases more or less as the square of the number of charges, leading to a roughly parabolic dependence of  $F$  on  $q$ , cf. Figures 4 and 5. At finite values of  $q$ ,  $F$  goes through a minimum with respect to  $R$  (cf. Figures 1–3). For small values of  $R$ , the value of  $F$  decreases with increasing  $R$ , due to the decrease of the strong electrostatic repulsions that exist for small  $R$  values.

One sees that, for small  $R$  values, the negative contribution of the derivative

$$\frac{\partial \beta F_q}{\partial R} = \frac{\partial \ln\langle \exp(\beta E) \rangle}{\partial R} \quad (4.3)$$

is not fully compensated by the positive contribution of the term, which incorporates the effects of diminishing the number of conformations while increasing  $R$  and thus extending the chain. This derivative is given by

$$\frac{\partial \beta F_0}{\partial R} = - \frac{\partial \ln(c_n(R))}{\partial R} \quad (4.4)$$

The latter term becomes dominant for larger values of  $R$ , so that there the slope of  $F$  with respect to  $R$  is positive. At the minimum of  $F$ , the influences of both effects are in balance. For increasing value of  $q$ , the average value of  $E$  increases, with a corresponding increase in the negative contribution of the term in eq 4.3. Consequently, the minimum in  $F$  shifts to larger values of  $R$ , and one sees that the chain expands on average. The same behavior can be seen in Figures 4 and 5, in the points where the curves for successive  $R$  values intersect each other, indicating that, in those points, a small change in the value of  $R$  has no effect on the value of  $F$ , thus indicating an extremum in  $F$ .

In Figures 4 and 5, one can clearly see a crossover appear in the behavior of the conformational free energy around a charge density of 50% (i.e., at the point where the segments are more or less alternately charged) and in particular for high values of  $R$ . At low values of  $q$ , the behavior of  $F$  resembles that of a quadratic function. Beyond 50% charge, the slope of the  $F(q)$  curve steeply increases. This same effect could be seen in Figures

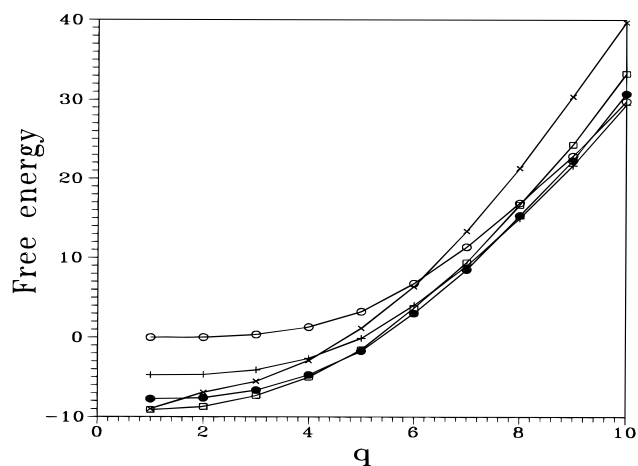


**Figure 4.** Conformational free energy (normalized by  $kT$ ) of a chain of 10 segments versus the total number of charges  $q$ , for fixed end-to-end distances  $R$  (normalized by  $a$ ), of (top to bottom) 1 ( $\times$ ), 3 ( $\square$ ), 5 ( $\bullet$ ), 7 ( $+$ ), and 9 ( $\circ$ ).  $\kappa a = 0.3$ .

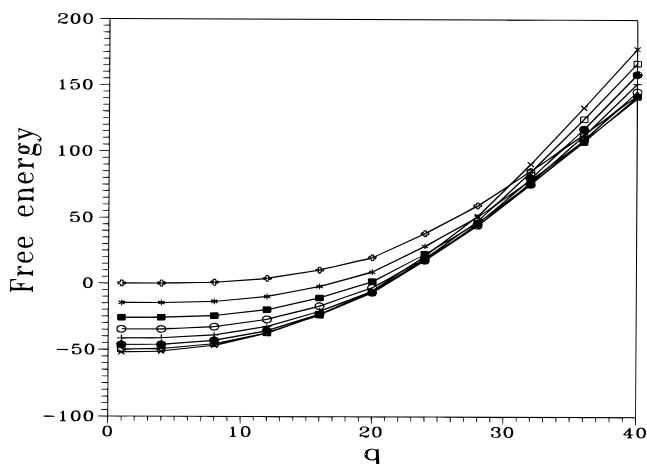


**Figure 5.** Conformational free energy (normalized by  $kT$ ) of a chain of 40 segments versus the total number of charges  $q$ , for fixed end-to-end distance  $R$  (normalized by  $a$ ), of (top to bottom) 11 ( $\times$ ), 15 ( $\square$ ), 19 ( $\bullet$ ), 23 ( $+$ ), 27 ( $\circ$ ), 31 ( $\blacksquare$ ), 35 ( $*$ ), and 39 ( $\star$ ).  $\kappa a = 0.3$ .

1–3, where the distance between the curves for different  $q$  values follows an arithmetic progression for low  $q$ , and above the transition (for a charge density of 60% and higher) the increase is more or less linear. For lower values of  $R$ , so for less strongly extended chains, this crossover is less pronounced. Clearly, this crossover does not result from the fact that the charges cannot be fixed completely equidistantly, as it persists above the crossover value for all values of  $q$ .

The point where the crossover between both types of behavior occurs is the point where the change in electrostatic and entropic contributions counterbalance upon extension. We see that, for longer chains, the position of this crossover becomes more well-defined. As one might expect, for increasing  $\kappa a$  this crossover shifts to higher charge densities due to the more effective screening (not shown). Note, however, that this effect is primarily of theoretical interest, as in this case counterion condensation will occur around 35% charge density.

A study of the influence of the charge interactions on the conformational free energy of the lattice polyelectrolyte is made by investigating the increase of this quantity due to charge interactions, defined by eq 2.8,

$$F_q(R, q, \kappa a, n) = F(R, q, \kappa a, n) - F_0(R, n) \quad (4.5)$$

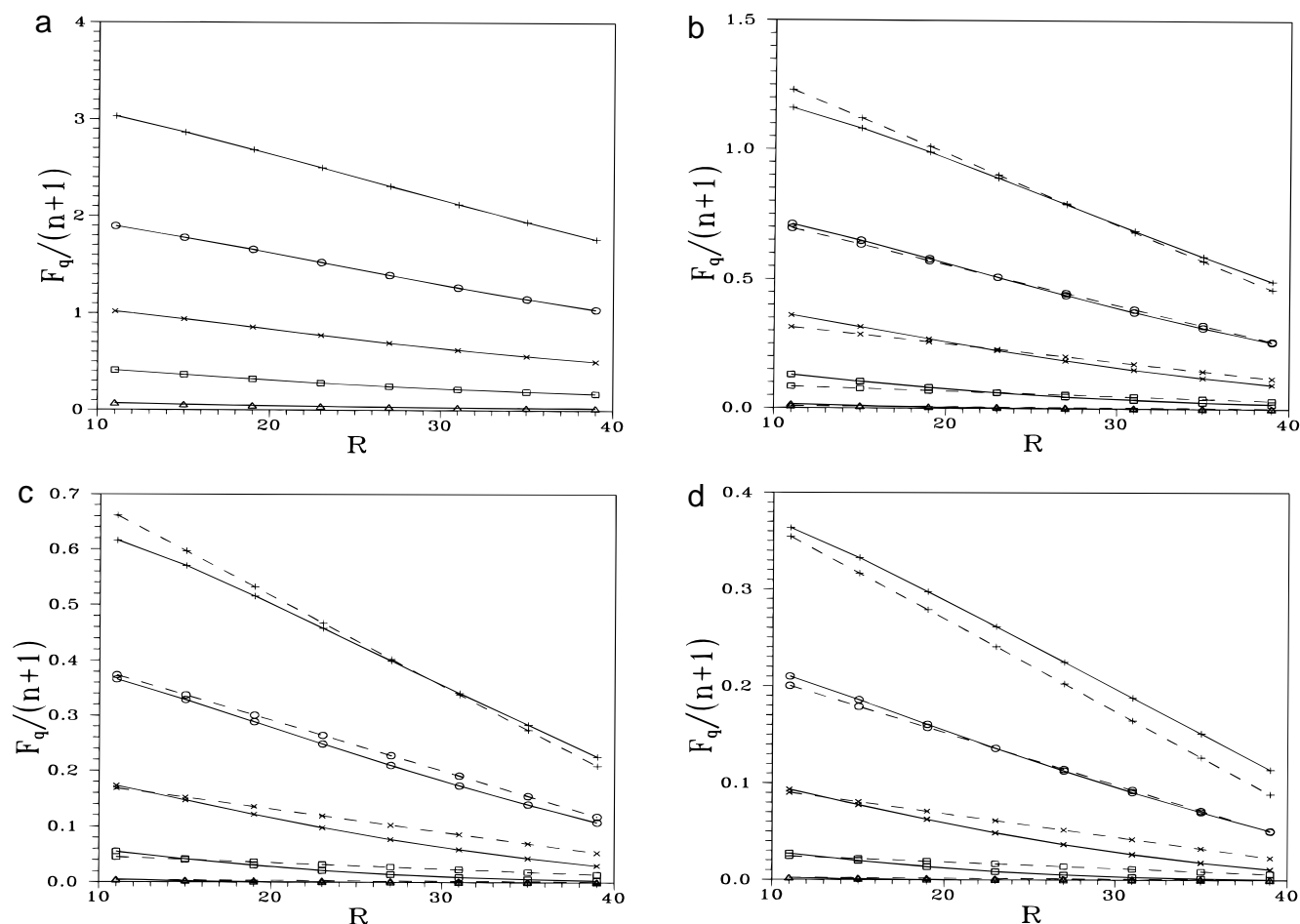


**Figure 6.** Plot of  $F_q/(n+1)$ , the increase of the free energy per segment due to charge interactions (in units  $kT$ ), versus  $R$  (normalized by  $a$ ), for different values of  $\kappa a$  and  $q$ , for a chain of 40 segments. Solid lines indicate the Monte Carlo results, and dashed lines represent the results obtained from eq 4.6.  $\kappa a =$  (a) 0, (b) 0.3, (c) 0.6, and (d) 0.9. For the different values of  $q$  we used the following symbols:  $q = 4$  ( $\Delta$ ), 8 ( $\square$ ), 12 ( $\times$ ), 16 ( $\circ$ ), and 20 ( $+$ ).

In Figure 6, the solid lines represent the electrostatic free energy increase per segment,  $F_q/(n+1)$  (in units  $kT$ ), versus the end-to-end distance  $R$  (normalized by  $a$ ), as calculated from the Monte Carlo data for a chain of 40 segments for  $q = 4, 8, 12, 16$ , and 20. The four graphs a–d represent respectively the data for the four values of  $\kappa$  used ( $\kappa a = 0, 0.3, 0.6$ , and  $0.9$ ).

From the Monte Carlo data, represented as solid curves in the graphs, we conclude that, for all values of  $\kappa a$  and particularly for the higher values of  $q$ ,  $F_q$  depends on  $R$  in an almost linear way. For  $\kappa a \geq 0.3$ , both the intercept and the slope of this linear relationship depend more or less exponentially on the value of  $\kappa a$ . For  $\kappa a = 0$ , this is not the case; the increase of the absolute value of the slope and the intercept for small  $\kappa a$  is much stronger than an exponential relationship would predict. Therefore, the Monte Carlo data for  $\kappa a \geq 0.3$ ,  $q \in \{2, \dots, 1/2(n+1)\}$  and  $R \geq 0.3na$  can be approximated by the following descriptive, analytical expression:

$$\frac{F_q(R, q, \kappa a, n)}{kT} = (n+1)A_1 \left[ \left( \frac{q}{n+1} \right)^2 + A_2 \left( \frac{q}{n+1} \right) + A_3 \right] \times \left[ \exp(-B_1 \kappa a) - C_1 \frac{R}{na} \exp(-B_2 \kappa a) \right] \quad (4.6)$$

Using the (arbitrary) weighing factor  $1/F_q^{1/2}$ , to somewhat enlarge the weight of the data points for low  $q$  values, we fitted our data to eq 4.6, for the four different chain lengths separately, and obtained for the coefficients the values given in Table 1. The reader should

**Table 1. Values of the Coefficients in Expression 4.6 for  $F_q$ , the Electrostatic Contribution to the Free Energy of a Lattice Polyelectrolyte with Fixed Endpoints, for  $\kappa a \geq 0.3$ ,  $0.1 \leq q/(n+1) \leq 0.5$ , and  $0.3na \leq R \leq na$**

coefficient	$n = 9$	$n = 19$	$n = 39$	$n = 79$
$A_1$	15.3	16.0	17.4	20.3
$A_2$	-0.34	-0.23	-0.20	-0.20
$A_3$	0.029	0.013	0.011	0.010
$B_1$	1.69	1.89	2.01	2.09
$B_2$	1.39	1.62	1.77	1.89
$C_1$	0.65	0.65	0.65	0.65

note that the coefficients for  $n = 9$  do not follow the general trend completely, as for these short chains the results for 0% charge density ( $q = 0$ ) and for 10% charge density ( $q = 1$ ) coincide. The results are plotted in Figures 6 (dashed lines). Approximate values for the coefficients for intermediate chain lengths can be obtained graphically by interpolation, provided the chain length chosen is not too short (see Figure 7). Furthermore, one should note that eq 4.6 does not behave correctly for  $q \rightarrow 0$ . Strictly speaking, the coefficient  $A_3$  should be equal to zero. However, we allow  $A_3$  to have finite values in order to obtain good fit results for the higher charge densities. For  $q < 2$ , we take  $F_q$  equal to zero, and for small  $q$  values ( $q \geq 2$ ), the relative differences between the outcome of eq 4.6 and the Monte Carlo data are somewhat larger, which is due to both the facts that, for low  $q$  values, the simulation curves are less straight and that the least-squares fitting method involves absolute instead of relative differences, which are typically small for small  $q$  values.

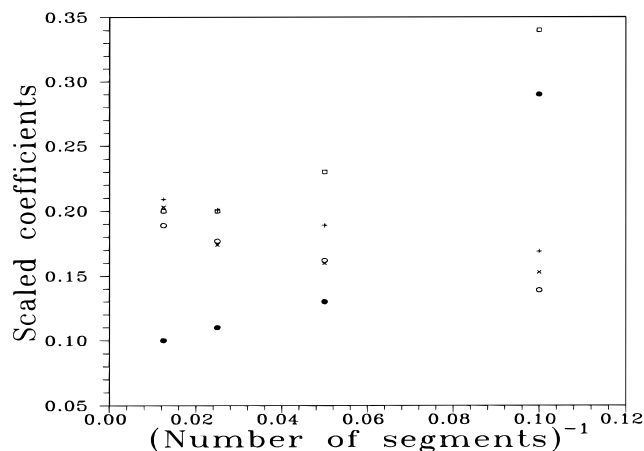


**Figure 7.** Coefficients of eq 4.6 versus the reciprocal number of segments,  $(n + 1)^{-1}$ . The coefficients are scaled in such a way that all scaled values fall between 0.1 and 1. Plotted are  $0.01A_1$  ( $\times$ ),  $-A_2$  ( $\square$ ),  $10A_3$  ( $\bullet$ ),  $0.1B_1$  ( $+$ ), and  $0.1B_2$  ( $\circ$ ). The constant coefficient  $C_1 = 0.65$  is not shown. Some of the coefficients approach a certain limiting value for  $n \rightarrow \infty$ .  $A_1$  is linear in the number of segments (not shown).

**Table 2. Values of the Cubic Fit Coefficients in the Expression for  $F_0$ , the Free Energy of an Uncharged Lattice Polyelectrolyte (See Eq 4.7)**

coefficient	$n = 9$	$n = 19$	$n = 39$	$n = 79$
$a'$	0.008201	0.8399	1.429	1.540
$b'$	1.690	0.4827	-0.3567	-0.4000
$c'$	-0.9001	-0.1521	0.3199	0.4000
$d'$	-0.7978	-1.171	-1.395	-1.540

The total free energy of the lattice polyelectrolyte is calculated by adding the entropic contribution of the uncharged SAW chain to the electrostatic part embodied in  $F_q$ . As for these short chains the scaling laws derived for  $c_n(R)$ , which are derived for long, continuous chains, do not apply,<sup>16</sup> we fitted this contribution to the following cubic function in  $R$ :

$$\frac{F_0(R, n)}{kT} = n \left[ a' \left( \frac{R}{na} \right)^3 + b' \left( \frac{R}{na} \right)^2 + c' \left( \frac{R}{na} \right) + d' \right] \quad (4.7)$$

The values for the fit coefficients obtained are presented in Table 2.

For all values of  $n$ , for  $R$  values  $0.3na \leq R \leq na$ , and for  $\kappa a \geq 0.3$ , eqs 4.6 and 4.7 give a good first approximation to the simulation data, particularly for high charge densities (*i.e.*, around and including Manning's condensation threshold). Given the number of fit parameters, the result for lower charge densities is somewhat discouraging. Nevertheless, the use of eqs 4.6 and 4.7 for predictive purposes, using inter- or extrapolated values of the fit parameters for chains with a different length, may have a certain practical usefulness. Below we shall discuss and derive an alternative expression which, though being less accurate, in particular for the highest charge densities, contains no fit parameters at all and, therefore, is more satisfactory from a theoretical point of view.

### 5. Comparison with Katchalsky's Theory

The theory of polyelectrolyte chains with fixed end-points which was developed by Katchalsky<sup>14,15</sup> is still by far the most widely used theory for the description of polyelectrolyte gels. In this section, we therefore compare our numerical results with Katchalsky's analytical result for the conformational free energy of a charged Gaussian chain with fixed end-to-end distance and screened Coulomb interactions between the charged

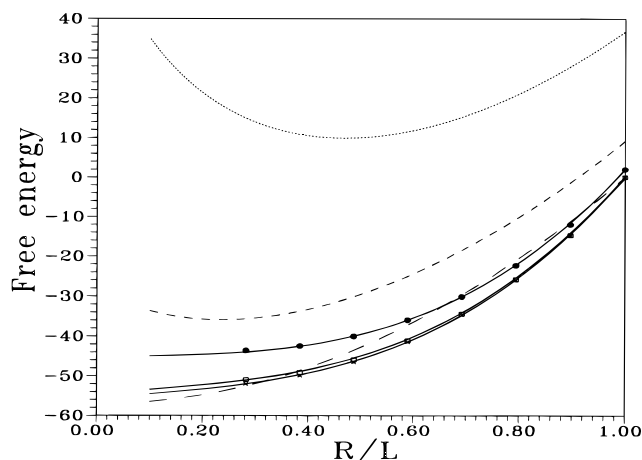


**Figure 8.** Conformational free energy of a chain of 40 segments (in units  $kT$ ) versus its relative extension ( $R/L$ ). Shown are the simulation results for a total number of 0 ( $\times$ ), 8 ( $\square$ ), and 16 ( $\bullet$ ) charges, the solid fitted curves (eqs 4.6 and 4.7) through the data points, and the corresponding curves of  $F(R)$ , as predicted by Katchalsky (eqs 5.2 and 5.3; 0 charges, long dashes; 8 charges, short dashes; 16 charges, dotted curve). For all curves,  $\kappa a = 0.9$ .

segments. For  $\kappa = 0$ , Katchalsky's result for the electrostatic free energy reads

$$\beta F_q(R) \approx \frac{q^2 Q}{R} \left[ 1 + \ln \left( \frac{3R^2}{2R_0^2} \right) \right] \quad (5.1)$$

which can only be valid for sufficiently large values of  $R$  (see Appendix 3). For "intermediate" values of  $\kappa$ , Katchalsky proposed

$$\beta F_q(R) \approx \frac{q^2 Q}{R} \ln \left[ 1 + 6 \frac{R}{\kappa R_0^2} \right] \quad (5.2)$$

where  $R_0$  is the mean square end-to-end distance of the uncharged Gaussian chain, for which  $R_0^2 = Nb^2$ , where  $N$  is the number of Kuhn segments of length  $b$ , and the length of the chain is given by  $L = Nb$ . The total free energy of the chain is calculated by addition of the electrostatic free energy and the elastic free energy of the uncharged Gaussian chain,

$$\beta F(R) = \beta F_q(R) + \frac{3}{2} \left[ \frac{R^2}{R_0^2} - 1 \right] \quad (5.3)$$

Katchalsky derived the results for  $F_q$  given in eqs 5.1 and 5.2 by averaging the electrostatic interactions of the charges on a Gaussian chain, assuming that the conformational behavior of this chain is not affected by the presence of these interactions (see Appendix 3). Due to this assumption, Katchalsky's theory predicts far too strong a dependence of the electrostatic free energy on the total charge, as we will show later. In our simulations, the Boltzmann factors of every conformation account in a correct way for the influence of the electrostatic interactions on the conformational behavior, by imparting a smaller weight to conformations of high electrostatic energy. The large errors that result if Katchalsky's assumption is adopted are shown in Figure 8, where we plotted, for 0%, 20%, and 40% charge densities, the  $F$  versus  $R$  curves as predicted by Katchalsky's theory and by our fit equation, for  $\kappa a = 0.9$ . Note that, at charge densities of about 35%, counterion condensation occurs.

To allow a comparison, we shifted all curves in such a way that the curves for zero charge ( $q = 0$ ) coincide at the point of complete extension ( $R = L$ ), according to our definition  $F(q = 0, R = L) = 0$ . Note that, implicitly, we assume the results for a lattice polyelectrolyte to be the same as those for a charged Gaussian chain. In the following we will show that differences due to this assumption are very small.

Qualitatively, both data sets show that the difference between the curves for  $q = 0$  and  $q = 8$  is much smaller than is the case for the curves for  $q = 8$  and  $q = 16$ , although the changes predicted by Katchalsky's formula are much larger than the simulation results suggest. For small values of  $R$  and  $q > 0$ , Katchalsky's model predicts much higher values for the conformational free energy and much steeper curves than the numerical results show. As the tensile force exerted by the polyion is given by the derivative of the conformational free energy with respect to  $R$ , Katchalsky's description predicts much stronger expansive forces at small  $R$ . Clearly, this arises from the overestimation of the influence of charge interactions in this model. In the simulations, a close approach of two charges is highly unlikely, which is reflected in the very small Boltzmann factor and thus a very small weight and influence of such a conformation on the chain behavior.

The extent of the overestimation of the charge interactions in Katchalsky's model strongly depends on the average segment density, and thus on the fixed end-to-end distance  $R$ . For small  $R$  values, many conformations show intersections. As these strongly contracted conformations contribute equally to the overall statistics of the system in Katchalsky's model, the predicted average value of  $R$  will be smaller, and consequently the corresponding minima of the conformational free energy with respect to  $R$  are, for low values of  $q$ , found at smaller values of  $R$  than those found in the simulation results. This implies that Katchalsky's model predicts less expanded dimensions at small charge densities, due to the absence of bare excluded volume and the strong contractile behavior of the Gaussian coil. Due to these conformations with small  $R$  values and consequently many intersections, an overestimation of the repulsive electrostatic interactions takes place in the case of high charge density, resulting in a strong increase of  $F$  with decreasing  $R$  values and a corresponding shift of the minimum in  $F$  to higher values of  $R$ . As a result, the model predicts a stronger average expansion at high charge densities than is observed in the simulation results.

In the figure, one can observe that, for small values of the extension, and in particular for high values of  $q$ , Katchalsky's model predicts a very strong increase of the conformational free energy. The numerical data for small  $n$  values also show this effect, but there it is much less pronounced. This can be explained by the fact that, for decreasing  $R$  values, the Gaussian chain shrinks as a whole, thereby giving rise to very high electrostatic interactions between its segments. The lattice polyelectrolyte will form more arclike conformations in this case, due to the fact that the chain statistics include the electrostatic repulsion. For higher values of  $n$  ( $> 19$ ), we could not confirm this behavior, as we did not obtain accurate results for very small  $R$  in a reasonable amount of time. Obtaining accurate simulation results at small  $R$  is difficult, as in this range the average segment density is high. This implies many undesired intersections, thus a small SAW fraction and high, strongly varying interaction energies, that lead to very large uncertainties in the value of  $\langle \exp(\beta E) \rangle$ . However, in a

**Table 3.** SAW Value of  $h_0$  To Be Used in Eqs 5.4c and 5.5

no. of segments ( $n + 1$ )	$h_0$
10	3.14
20	4.93
40	7.59
80	11.6

swollen gel, this aspect is not important, as very small  $R$  values are not likely to occur.

To obtain a more satisfactory description of the electrostatic free energy of a polyelectrolyte with fixed endpoints, we extended Katchalsky's treatment (see Appendix 3) and propose a simplification of the partition sum, in which the influence of all pair interactions between charged segments on the conformational statistics of the Gaussian chain are taken into account but correlations between different charge pairs are neglected.

For  $q < 2$ , we find for the partition sum (normalized by the partition sum of the uncharged chain)

$$Z(R, q, \kappa) = 1 \quad (5.4a)$$

which corresponds to an electrostatic contribution to the free energy of zero. For  $q = 2$ , only the fixed endpoints are charged, and we find

$$Z(R, q, \kappa) = \exp \left\{ - \frac{Q \exp(-\kappa R)}{R} \right\} \quad (5.4b)$$

For  $2 < q \leq n$ , the result is given by

$$Z(R, q, \kappa) = \exp \left\{ - \frac{Q \exp(-\kappa R)}{R} \right\} \prod_{k=1}^{q-2} \left[ \int_0^\infty \exp \left\{ - \frac{Q \exp(-\kappa r)}{r} \right\} \times W \left( \frac{k}{q-1}, r, R \right) dr \right]^{q-k} \quad (5.4c)$$

where the function  $W(k/(q-1), r, R)$  is the probability distribution of the spatial distance  $r$  of two charges, residing at a fixed contour distance  $kL/(q-1)$  on the Gaussian chain, the endpoints of which are fixed at a spatial distance  $R$  of each other. Taking the natural logarithm gives the corresponding electrostatic contribution to the free energy (see eq 2.6). If the scaled parameters  $Q/h_0$ ,  $\kappa h_0$ ,  $R/h_0$ , and  $r/h_0$  are used instead of  $Q$ ,  $\kappa$ ,  $R$ , and  $r$ , respectively, where  $h_0$  is the most probable value of the endpoint distance of the uncharged Gaussian chain ( $h_0^2 = (2/3)R_0^2$ ), expressions 5.4a–c remain unchanged, and the expression for  $W$  simplifies to

$$W(\xi, r, R) = [\pi \xi (1 - \xi)]^{-1/2} \frac{r}{R \xi} \left\{ \exp \left[ - \frac{(r - R \xi)^2}{\xi (1 - \xi)} \right] - \exp \left[ - \frac{(r + R \xi)^2}{\xi (1 - \xi)} \right] \right\} \quad (5.5)$$

Note that, in Appendix 3, we followed Katchalsky's notation and used  $h$  instead of  $R$ .  $\xi$  is a short notation for  $k/(q-1)$ . In Table 3, we present the values of  $h_0$  to be used for the chain lengths studied, which are calculated from the values for the mean square end-to-end distance  $R_0^2$  of self-avoiding walks,<sup>8</sup> by multiplying by  $2/3$  and taking the square root. We use this method because, in the calculation of eqs 5.4a–c, the distribution function of the chain segments is approximated by a Gaussian function. The parameters of this function should be chosen in such a way that, for zero charge,

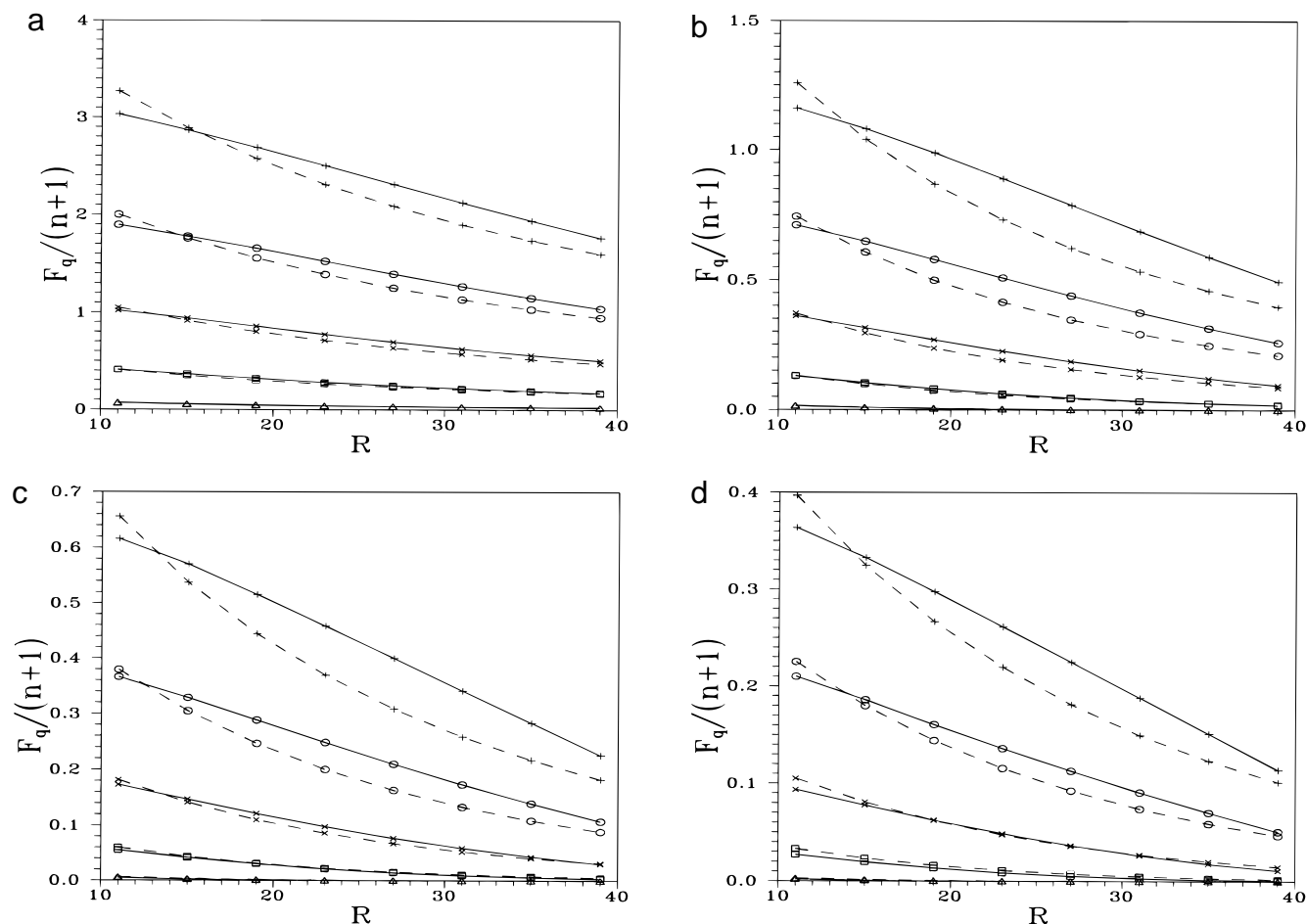


**Figure 9.** Plot of  $F_q/(n+1)$ , the increase of the free energy per segment due to charge interactions (in units  $kT$ ), versus  $R$  (normalized by  $a$ ), for different values of  $q$  and  $\kappa a$ , for a chain of 40 segments. Simulation data (solid line) are plotted, together with the numerical results according to eqs 5.4a–c (dashed line), in the same way as in Figure 6a–d.

the results reduce to those of an uncharged lattice chain. Therefore, the mean square end-to-end distance must be set equal to the value for a self-avoiding walk.

To check the validity of eqs 5.4a–c, we present, in Figure 9, the results of these expressions for the electrostatic free energy of a chain of 40 segments together with the simulation data, in the same way as we did in Figure 6.

The result obtained is very satisfactory. For charge densities up to 30%, the values calculated by means of eqs 5.4a–c are in good agreement with the simulation results. As the condensation threshold according to Manning is reached at about 35% charge density (for the values of the parameters chosen), this means that over almost the entire range of experimentally accessible parameter values, the expressions 5.4a–c give quite satisfactory results.

At and around the condensation threshold, we see that the almost linear relationship between  $F_q$  and the extension  $R$ , which shows up in the simulation results, is not represented well by eqs 5.4. For relatively high charge densities, the description by means of eq 4.6, giving more accurate results, might, therefore, be preferred.

Finally, to present a clear view on the improvement made by the introduction of charge pair interactions on the chain statistics in Katchalsky's theory, we plotted, in Figure 10, the results for  $F_q/(n+1)$ , the electrostatic free energy increase per segment, the simulation results, the results from eqs 5.4a–c, and the results according to Katchalsky (eq 5.2) for  $\kappa a = 0.3$ , for a chain of 40 segments as a function of the fixed end-to-end distance  $R$ , normalized by the segment length  $a$ .

Clearly, the values for the free energy predicted by Katchalsky's formula are much higher than those of the other two data sets. Besides, Katchalsky's expression and, to a lesser extent, expressions 5.4a–c show a much stronger dependence on  $R$  than the simulation results, in particular for high values of the charge density and for small values of  $R$ . As discussed, this strong increase of  $F$  is due to taking conformations with unrealistic high electrostatic energies into account in the averaging process. The improvement of eq 5.4 over eq 5.2 is thus caused by the incorporation of the effect of charge pair interactions on the conformation distribution function of the segments. For a small (20%) charge density, the agreement between the simulation results and the outcome of eq 5.4 is very good, indicating that both the adoption of a Gaussian segment distribution and the neglect of higher order charge interactions cause only relatively small errors compared to the simulation data. For high charge densities, the neglect of the effect of higher order charge interactions introduces too large a weight of conformations of high energy, resulting in too high  $F$  values for small  $R$ . Precisely, these higher order charge effects on the segment–segment distribution function (which become more dominant at higher charge densities) must be responsible for the strong linear relationship between  $F_q$  and  $R$  found at high charge densities in the simulation results.

## 6. Conclusions

The Monte Carlo data obtained for the conformational free energy of lattice polyelectrolytes with fixed end-points reveal that the dependence of  $F_q$ , the electrostatic contribution to this free energy, on the number of chain



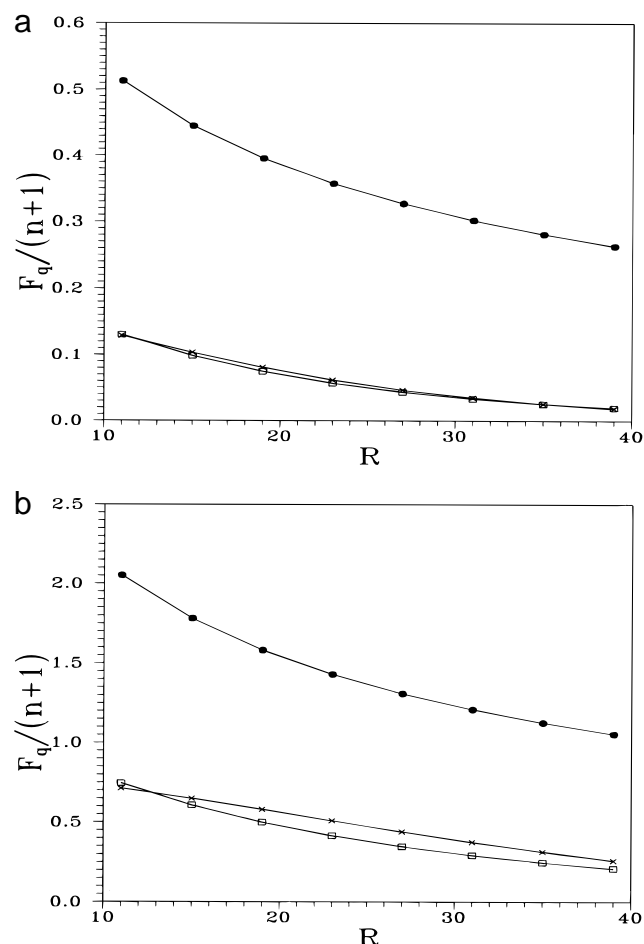


**Figure 10.** Comparison between different predictions for the electrostatic free energy per segment,  $F_q/(n+1)$  (in units  $kT$ ), versus the end-to-end distance  $R$  (normalized by  $a$ ), for a representative choice of parameters:  $\kappa a = 0.3$ ,  $n = 39$ , and for two values of the charge density: (a)  $q = 8$  (20% charge density) and (b)  $q = 16$  (40% charge density). Shown are the simulation results ( $\times$ ), results calculated using eqs 5.4 ( $\square$ ), and results from Katchalsky's formula, eq 5.2 ( $\bullet$ ).

segments  $n$ , the total charge  $q$ , the inverse Debye screening length  $\kappa$ , and the fixed end-to-end distance  $R$  differs strongly from the form usually assumed (see, for instance, eqs 5.1 and 5.2 and Figure 8). For predictive purposes, we propose a simple analytical expression that gives a good estimate (see Figure 6) of the conformational free energy of a lattice polyelectrolyte with fixed endpoints, in particular for high charge densities (*i.e.*, at and around Manning's condensation threshold). This expression contains a considerable number of fit parameters, which are given, and which may be inter- or extrapolated for chains of different lengths.

By a thorough investigation of the derivation of Katchalsky's result (see Appendix 3), it is found that the discrepancies between the Monte Carlo data and his prediction are caused mainly by the fact that the electrostatic free energy is simply averaged over all conformations of the Gaussian chain (see eq A3.7), instead of using in the averaging process the relative weights (given by the appropriate Boltzmann factors) of these conformations. We therefore propose a simplified version of the partition sum (see eqs 5.4), which incorporates charge pair interactions. For all chain lengths, end-to-end distances, values of the Debye length studied, and for not too high charge densities, the agreement between the Monte Carlo data and the free energy resulting from this expression is very good (see Figure 9). As this expression contains no fit

parameter (though it still contains an integral), it is more convenient, in addition to giving more insight into the statistics of the chain. In particular, one may conclude that neglecting higher order charge correlations is reasonably appropriate for this system. Theories alternative to Katchalsky's to calculate the electrostatic free energy of polyelectrolytes with fixed endpoints have not really been given.

**Acknowledgment.** One of the authors acknowledges support by the Koninklijke/Shell Laboratories, Amsterdam.

## Appendix 1

The derivation of the endpoint distribution of a random walk (RW) of  $n$  steps is performed by calculating the number of conformations this RW can attain while its endpoints are fixed. We assume that the RW starts in the origin and ends, after  $n$  steps, in  $\mathbf{R}(x, y, z)$ .

**Simple Random Walks.** A RW of  $n$  steps on a  $d$ -dimensional cubic lattice is a series of  $n$  unit steps in one of the  $2d$  perpendicular directions (a step in the positive  $x$ -direction is not the same as a step in the negative  $x$ -direction). By writing the steps of a particular RW in the order in which they are taken, every RW is uniquely defined. Denoting the direction of the  $k$ th step by  $i_k$ , where  $i_k \in \{-x, +x, -y, +y, -z, +z\}$ , any particular RW can be represented by the set  $\{i_k\}$ , and the following general expression for the endpoint distribution of any self-intersecting lattice walk can be used:

$$P(\mathbf{R}) = \sum_{\{i_1, \dots, i_n\}} \phi(i_1, \dots, i_n) \delta(\mathbf{R} - \sum_{k=1}^n \mathbf{u}_{i_k}) \quad (\text{A1.1})$$

where the function  $\phi$  gives the probability of the occurrence of a certain conformation in terms of the *directions* of the individual bond vectors  $\mathbf{u}_{i_k}$ , the summation over  $\{i_1, \dots, i_n\}$  is performed over *all* possible combinations of the  $i_k$ , *i.e.*, over all conformations the RW can attain, and the Kronecker  $\delta$  function ensures that only conformations with the desired end-to-end distance are counted. For the continuous case, one should take a Dirac  $\delta$  function, and the function  $\phi$  would be a probability density distribution, but the general shape of the equation would be the same.

The function  $\phi$  depends on the constraints set for neighboring steps. For an ordinary RW on a cubic lattice, for which consecutive steps are not correlated, all conformations have the same probability, and one obtains

$$\phi(i_1, \dots, i_n) = \frac{1}{(2d)^n} \quad (\text{A1.2})$$

For the simple case of a regular one-dimensional ( $d = 1$ ) RW, which consists of  $n$  steps along the  $x$ -axis, we thus find

$$\begin{aligned} P(x) &= \sum_{\{i_1, \dots, i_n\}} \frac{1}{2^n} \delta(x - \sum_{m=1}^n u_{i_m}) \\ &= \frac{1}{2^n} \sum_{\{i_1, \dots, i_n\}} \frac{1}{2^n} \sum_k \exp[ik(x - \sum_{m=1}^n u_{i_m})] \end{aligned} \quad (\text{A1.3})$$

where we used a discrete Fourier representation of the Kronecker  $\delta$  function. We find

$$\begin{aligned} P(x) &= \frac{1}{2^n} \frac{1}{2\pi} \sum_k \exp(-ikx) \sum_{\{i_1, \dots, i_n\}} \exp[ik \sum_{m=1}^n u_{i_m}] \\ &= \frac{1}{2^n} \frac{1}{2\pi} \sum_k \exp(-ikx) \sum_{\{i_1, \dots, i_n\}} \prod_{m=1}^n \exp(iku_{i_m}) \end{aligned} \quad (\text{A1.4})$$

Equation A1.4 involves the summation over all possible multiplications of imaginary exponentials. As there are only two possible values for the  $u_i$  (e.g.,  $-1$  and  $+1$ ), all possible combinations of multiplications of  $n_-$  factors  $\exp(-ik)$  and  $n_+$  factors  $\exp(+ik)$ , under the constraint that  $n_- + n_+ = n$ , are to be summed. For this we can use the binomial theorem, which states that  $(\exp(ik) + \exp(-ik))^n$  contains all these combinations, so

$$P(x) = \frac{1}{2^n} \frac{1}{2\pi} \sum_k \exp(-ikx) [\exp(ik) + \exp(-ik)]^n \quad (\text{A1.5})$$

Using the binomial theorem again, rearranging the result, and transforming back to an expression containing a Kronecker  $\delta$  function (only contributing if the argument is zero), we find

$$\begin{aligned} P(x) &= \frac{1}{2^n} \frac{1}{2\pi} \sum_k \exp(-ikx) \sum_{p=0}^n \binom{n}{p} e^{ikp} e^{ik(n-p)} \\ &= \frac{1}{2^n} \sum_{p=0}^n \binom{n}{p} \sum_k e^{-ik(x-2p+n)} \\ &= \frac{1}{2^n} \sum_{p=0}^n \binom{n}{p} \delta\left(p - \frac{x+n}{2}\right) \\ &= \frac{1}{2^n} \binom{n}{1/2(x+n)} \end{aligned} \quad (\text{A1.6})$$

where

$$\binom{n}{k} \equiv \frac{n!}{k!(n-k)!} \quad (\text{A1.7})$$

provided that  $n$  and  $k$  are nonnegative integers and  $k \leq n$ . Otherwise, the outcome is zero.

For a three-dimensional RW, we can follow essentially the same route. The 3d equivalent of eq A1.3 becomes

$$P(\mathbf{R}) = \sum_{\{i_1, \dots, i_n\}} \frac{1}{6^n} \delta(\mathbf{R} - \sum_{m=1}^n \mathbf{u}_{i_m}) \quad (\text{A1.8})$$

The 3d expression for the Kronecker  $\delta$  function, involving the dot product  $\mathbf{k} \cdot \mathbf{R}$ , can be factorized,

$$\begin{aligned} P(\mathbf{R}) &= \frac{1}{(2\pi)^3} \frac{1}{6^n} \sum_{k_x} e^{-ik_x x} \sum_{k_y} e^{-ik_y y} \sum_{k_z} e^{-ik_z z} \times \\ &\quad \sum_{\{i_1, \dots, i_n\}} \prod_{m=1}^n \exp[i\mathbf{k} \cdot \mathbf{u}_{i_m}] \end{aligned} \quad (\text{A1.9})$$

Again, the summation of all multiplications of imaginary exponents of the components of  $\mathbf{k}$ , corresponding

to the steps taken by all possible RWs, can conveniently be written in the form

$$P(\mathbf{R}) = \frac{1}{(2\pi)^3} \frac{1}{6^n} \sum_{k_x} e^{-ik_x x} \dots \sum_{k_z} e^{-ik_z z} [e^{ik_x} + e^{-ik_x} + e^{ik_y} + e^{-ik_y} + e^{ik_z} + e^{-ik_z}]^n \quad (\text{A1.10})$$

Using the binomial theorem twice, we obtain a result similar to the one in eq A1.6:

$$\begin{aligned} P(\mathbf{R}) &= \frac{1}{6^n} \sum_{p=0}^n \binom{n}{p} \frac{1}{2\pi} \sum_{k_x} e^{-ik_x x} (e^{ik_x} + e^{-ik_x})^{n-p} \sum_{q=0}^p \binom{p}{q} \times \\ &\quad \frac{1}{2\pi} \sum_{k_y} e^{-ik_y y} (e^{ik_y} + e^{-ik_y})^{p-q} \sum_{q=0}^p \binom{p}{q} \frac{1}{2\pi} \sum_{k_z} e^{-ik_z z} (e^{ik_z} + e^{-ik_z})^{p-q} \end{aligned} \quad (\text{A1.11})$$

The calculation is analogous to eqs A1.5 and A1.6, and we obtain

$$\begin{aligned} P(\mathbf{R}) &= \frac{1}{6^n} \sum_{p=0}^n \binom{n}{p} \binom{n-p}{1/2(n-p+x)} \times \\ &\quad \sum_{q=0}^p \binom{p}{q} \binom{q}{1/2(q+y)} \binom{p-q}{1/2(p-q+z)} \end{aligned} \quad (\text{A1.12})$$

for the end-to-end distribution function of a 3d RW on a cubic lattice. The walk starts in the origin  $\mathbf{O}(0,0,0)$  and ends in  $\mathbf{R}(x,y,z)$ . In the course of the calculation, only local properties of the RW under consideration are taken into account explicitly in the function  $\phi$ . The steps set in the course of the walk are Fourier-transformed to exponential factors (e.g.,  $\exp(ik_x)$  for a step in the positive  $x$ -direction), which only have to agree with the constraints set between successive steps of the walk. The commutative property of the resulting multiplication makes it possible to rearrange the result into a simple form and to transform back to the Kronecker  $\delta$  function, which eventually is summed. The global constraint, i.e., the fact that all steps together must result in the desired endpoint vector, is automatically taken care of by the original Kronecker  $\delta$  function. As a corollary, it is not possible to use the same method to calculate the endpoint distribution of a self-avoiding walk, as for this type of walk the constraint pertains to all the lattice points visited and not only to neighboring steps.

Equation A1.12 can be simplified a bit to

$$\begin{aligned} P(\mathbf{R}) &= \frac{1}{6^n} \sum_{p=0}^n \binom{n}{p} \binom{n-p}{1/2(n-p+x)} \binom{p}{1/2(p+z+y)} \times \\ &\quad \binom{p}{1/2(p+z-y)} \end{aligned} \quad (\text{A1.13})$$

This is the probability of an  $n$ -step RW starting in the origin  $\mathbf{O}(0,0,0)$  and ending in  $\mathbf{R}(x,y,z)$ . The number of possible conformations is this probability, multiplied by

**Table 4. Free Energy of a Lattice Polyelectrolyte of 10 Segments**

$q$	$R=1$	$R=3$	$R=5$	$R=7$	$R=9$
A. Results for $n=10$ and $\kappa a=0.0$					
0	-8.99	-9.10	-7.75	-4.72	0.000
2	-6.21	-8.17	-7.19	-4.32	0.310
3	-3.60	-5.58	-5.08	-2.71	1.56
4	0.878	-1.45	-1.38	0.367	4.02
5	7.50	4.48	3.94	5.13	8.02
6	15.8	12.8	11.7	12.3	14.4
7	26.6	22.1	20.7	20.5	22.1
8	38.9	33.6	31.7	30.4	31.5
9	53.1	45.9	43.0	41.4	41.6
10	68.0	60.4	56.8	54.4	53.7
B. Results for $n=10$ and $\kappa a=0.3$					
0	-8.99	-9.10	-7.75	-4.72	0.000
2	-6.93	-8.72	-7.63	-4.67	0.021
3	-5.51	-7.32	-6.65	-4.09	0.355
4	-2.91	-5.00	-4.70	-2.65	1.31
5	1.17	-1.53	-1.70	-0.094	3.25
6	6.37	3.70	3.05	4.07	6.79
7	13.4	9.44	8.53	8.99	11.4
8	21.3	16.7	15.3	15.0	16.9
9	30.4	24.2	22.2	21.6	22.8
10	39.7	33.2	30.7	29.3	29.8
C. Results for $n=10$ and $\kappa a=0.6$					
0	-8.99	-9.10	-7.75	-4.72	0.000
2	-7.46	-8.94	-7.72	-4.71	0.001
3	-6.65	-8.15	-7.24	-4.49	0.092
4	-5.08	-6.76	-6.15	-3.76	0.487
5	-2.50	-4.64	-4.34	-2.26	1.54
6	0.951	-1.21	-1.28	0.364	3.74
7	5.65	2.69	2.39	3.66	6.84
8	11.0	7.54	6.85	7.61	10.5
9	17.1	12.6	11.5	12.1	14.4
10	23.3	18.6	17.1	17.0	18.8
D. Results for $n=10$ and $\kappa a=0.9$					
0	-8.99	-9.10	-7.75	-4.72	0.000
2	-7.86	-9.04	-7.74	-4.72	0.000
3	-7.36	-8.56	-7.50	-4.63	0.025
4	-6.39	-7.70	-6.86	-4.24	0.192
5	-4.72	-6.37	-5.73	-3.32	0.786
6	-2.37	-4.05	-3.68	-1.59	2.24
7	0.894	-1.29	-1.12	0.738	4.46
8	4.65	2.09	1.94	3.48	7.00
9	8.86	5.57	5.22	6.56	9.74
10	13.1	9.72	9.04	9.92	12.6

the total number of conformations:  $6^n$ . Thus, we find for  $c_n(R)$  of a RW

$$c_n(R) = \sum_{p=0}^n \binom{n}{p} \binom{n-p}{1/2(n-p+x)} \binom{p}{1/2(p+z+y)} \times \binom{p}{1/2(p+z-y)} \quad (\text{A1.14})$$

## Appendix 2

Table 4 lists the free energy (in units  $kT$ ) of a lattice polyelectrolyte of 10 segments, with total charge  $q$  and fixed end-to-end distance  $R$ , for four different values of  $\kappa a$ .

Table 5 lists the free energy (in units  $kT$ ) of a lattice polyelectrolyte of 20 segments, with total charge  $q$  and fixed end-to-end distance  $R$ , for four different values of  $\kappa a$ .

Table 6 lists the free energy (in units  $kT$ ) of a lattice polyelectrolyte of 40 segments, with total charge  $q$  and fixed end-to-end distance  $R$ , for four different values of  $\kappa a$ .

Table 7 lists the free energy (in units  $kT$ ) of a lattice polyelectrolyte of 80 segments, with total charge  $q$  and fixed end-to-end distance  $R$ , for four different values of  $\kappa a$ .

## Appendix 3

Katchalsky derived a well-known expression for the electrostatic free energy of a polyelectrolyte with fixed endpoints<sup>14</sup> by assuming that the conformational statistics of a Gaussian chain do not change (much) when this chain is charged. Clearly, this assumption will only be more or less valid if the charge interactions are of a weak and short-ranged nature, *i.e.*, in the case of a small number of charges and a strong Debye screening. Nevertheless, for  $\kappa = 0$ , a result is also presented,

$$\frac{F_q(h)}{kT} = \frac{q^2 Q}{h} \left[ 1 + \ln \left( \frac{h^2}{h_0^2} \right) \right] \quad (\text{A3.1})$$

where  $h$  is the fixed end-to-end distance of the polyion,  $h_0$  is its most probable end-to-end distance in the uncharged case, and  $q$  and  $Q$  denote the number of charges on the chain and the Bjerrum length, respectively. Close examination of this result shows that, for  $h/h_0 < 0.5e^{-1}$ , the electrostatic free energy becomes *negative*, which is quite contrary to the strong increase of this quantity to be expected if a charged chain is compressed. We therefore give a derivation of this expression to show its limited validity.

Katchalsky calculated the electrostatic part of the conformational free energy of a charged Gaussian chain by averaging the electrostatic interaction of all charge pairs over all conformations the chain can attain while its end-to-end distance is fixed. First, an expression is derived for the probability distribution  $W(N, k, \mathbf{r}, \mathbf{h})$  of the vectorial distance  $\mathbf{r}$  of two (charged) segments, located a certain number ( $k$ ) of segments apart along the contour of the chain, with the constraint that the (fixed) end-to-end vector of the chain is  $\mathbf{h}$  and the chain length  $L$  is equal to  $NA$ . Here,  $N$  is the number of segments of length  $A$  that constitute the chain.  $W$  can be calculated using the vectorial end-to-end distribution  $P(N, \mathbf{h})$  of a Gaussian chain,

$$P(N, \mathbf{h}) = \left( \frac{3}{2\pi NA^2} \right)^{3/2} \exp \left\{ -\frac{3\mathbf{h}^2}{2NA^2} \right\} \quad (\text{A3.2})$$

where  $\mathbf{h}$  is its end-to-end vector. For the calculation of  $W(N, k, \mathbf{r}, \mathbf{h})$ , the Gaussian chain is considered to consist of two subchains, the first of which is of length  $kA$  and governs the distance between the charged segments, which are located at its endpoints. The other subchain has length  $(N-k)A$ . It starts in the endpoint of the first chain, and its other endpoint is positioned in such a way that the endpoint vector of the total chain is  $\mathbf{h}$ . For the conditional probability  $W$  one then obtains the following expression:

$$W(N, k, \mathbf{r}, \mathbf{h}) = \frac{P(k, \mathbf{r}) P(N-k, \mathbf{h}-\mathbf{r})}{P(N, \mathbf{h})} \quad (\text{A3.3})$$

where the division is due to the condition of fixed end-to-end distance  $\mathbf{h}$ . As one can see, one of the segments

Table 5. Free Energy of a Lattice Polyelectrolyte of 20 Segments

$q$	$R = 1$	$R = 3$	$R = 5$	$R = 7$	$R = 9$	$R = 11$	$R = 13$	$R = 15$	$R = 17$	$R = 19$
A. Results for $n = 20$ and $\kappa a = 0.0$										
0	-23.2	-23.5	-23.2	-22.4	-20.9	-18.7	-15.6	-11.5	-6.41	0.000
2		-22.6	-22.7	-22.0	-20.6	-18.4	-15.4	-11.4	-6.25	0.147
4		-17.9	-18.3	-18.1	-17.2	-15.5	-12.8	-9.13	-4.28	1.90
6		-8.60	-9.49	-9.83	-9.56	-8.49	-6.47	-3.43	0.831	6.49
8		5.06	3.56	2.65	2.30	2.68	3.91	6.14	9.56	14.4
10			20.4	18.9	18.0	17.6	18.0	19.3	21.7	25.5
12			42.9	40.7	39.3	38.2	37.8	38.3	39.8	42.7
14			68.7	65.6	63.4	61.6	60.4	59.9	60.4	62.5
16			101	96.8	93.6	91.0	88.9	87.4	86.7	87.9
18			136	130	126	122	119	116	114	114
20			175	168	162	157	153	149	146	145
B. Results for $n = 20$ and $\kappa a = 0.3$										
0	-23.2	-23.5	-23.2	-22.4	-20.9	-18.7	-15.6	-11.5	-6.42	0.000
2	-21.1	-23.2	-23.1	-22.4	-20.9	-18.7	-15.6	-11.5	-6.42	0.001
4	-19.0	-21.0	-21.3	-20.9	-19.8	-17.9	-15.0	-11.1	-6.12	0.211
6	-14.2	-16.6	-17.2	-17.2	-16.6	-15.1	-12.7	-9.21	-4.59	1.41
8	-6.90	-9.74	-10.8	-11.2	-11.0	-10.0	-8.13	-5.24	-1.19	4.27
10	2.83	-0.895	-2.44	-3.21	-3.41	-2.96	-1.66	0.588	3.95	8.67
12	15.8	11.4	9.58	8.41	7.83	7.80	8.56	10.2	13.0	17.1
14	31.5	25.4	22.6	21.3	20.3	19.9	20.1	21.1	23.2	26.9
16	49.4	42.8	39.9	37.7	36.4	35.6	35.2	35.4	36.8	39.7
18	70.3	61.1	57.4	54.8	52.9	51.5	50.6	50.1	50.7	52.7
20	91.5	83.5	77.7	74.1	71.8	69.7	67.9	66.6	66.2	67.3
C. Results for $n = 20$ and $\kappa a = 0.6$										
0	-23.2	-23.5	-23.2	-22.4	-20.9	-18.7	-15.6	-11.5	-6.42	0.000
2	-21.7	-23.4	-23.2	-22.4	-20.9	-18.7	-15.6	-11.5	-6.42	0.000
4	-20.6	-22.3	-22.3	-21.8	-20.5	-18.4	-15.4	-11.4	-6.36	0.032
6	-18.0	-19.9	-20.2	-19.9	-18.9	-17.1	-14.4	-10.6	-5.79	0.425
8	-13.8	-16.0	-16.5	-16.5	-15.8	-14.3	-12.0	-8.59	-4.10	1.76
10	-8.08	-10.8	-11.7	-11.9	-11.5	-10.3	-8.31	-5.37	-1.33	4.03
12	-0.012	-3.07	-4.06	-4.49	-4.35	-3.54	-1.89	0.694	4.37	9.40
14	9.73	5.58	4.22	3.68	3.59	4.10	5.36	7.58	10.9	15.8
16	20.7	16.4	15.0	14.2	14.0	14.2	15.0	16.7	19.5	23.9
18	33.1	27.6	25.7	24.9	24.4	24.4	24.9	26.1	28.4	32.1
20	45.7	40.2	38.1	36.8	36.1	35.7	35.7	36.3	38.0	41.0
D. Results for $n = 20$ and $\kappa a = 0.9$										
0	-23.2	-23.5	-23.2	-22.4	-20.9	-18.7	-15.6	-11.6	-6.43	0.000
2		-23.5	-23.2	-22.4	-20.9	-18.7	-15.6	-11.6	-6.43	0.000
4		-22.9	-22.8	-22.1	-20.7	-18.6	-15.5	-11.5	-6.41	0.005
6		-21.5	-21.6	-21.1	-19.9	-17.9	-15.0	-11.2	-6.18	0.141
8		-19.1	-19.3	-19.0	-18.0	-16.3	-13.6	-10.0	-5.28	0.803
10		-15.9	-16.3	-16.2	-15.4	-13.8	-11.4	-8.11	-3.68	2.04
12		-10.6	-11.1	-11.2	-10.6	-9.28	-7.11	-4.00	0.206	5.75
14		-4.68	-5.38	-5.55	-5.17	-4.09	-2.15	0.736	4.79	10.2
16		2.68	1.93	1.64	1.86	2.71	4.34	6.90	10.6	15.7
18		10.2	9.29	8.94	9.03	9.65	11.0	13.3	16.6	21.4
20		18.4	17.3	16.9	16.9	17.2	18.2	20.0	22.9	27.2

under consideration, is by definition, located at one end of the chain, but as the chain is Gaussian, it can be shown that the result is the same as for the more general case (of three subchains, the middle one governing the distance between the charges, which are located somewhere along the contour, and both of the outer chains maintaining the fixed end-to-end distance). The expression for  $P(N, \mathbf{h})$  is substituted in eq A3.3. Denoting the square of the most probable value of the end-to-end distance of the uncharged molecule by  $h_0^2$  ( $\equiv 2NA^2/3$ ) and defining  $\xi \equiv k/N$ , the result becomes

$$W(\xi, \mathbf{r}, \mathbf{h}) = [\pi h_0^2 \xi (1 - \xi)]^{-3/2} \times \exp \left\{ \frac{\mathbf{h}^2}{h_0^2} - \frac{\mathbf{r}^2}{h_0^2 \xi} - \frac{(\mathbf{h} - \mathbf{r})^2}{h_0^2 (1 - \xi)} \right\} \quad (\text{A3.4})$$

where we omitted the parameter  $N$  (now included in  $h_0^2$ ) to stress the difference between  $W$  and  $\bar{W}$ . For our calculation, only the scalar dependence on  $r$  is relevant. We therefore multiply by the volume element  $r^2 dr d\varphi d\cos\theta$  and integrate over both angles. For convenience,  $\mathbf{h}$  is chosen in the  $z$ -direction. Only the last term in the exponent, containing  $2hr\cos\theta$ , gives a nonconstant

contribution, and, rearranging, we obtain Katchalsky's result,

$$W(\xi, r, h) = [\pi h_0^2 \xi (1 - \xi)]^{-1/2} \frac{r}{h\xi} \left\{ \exp \left[ -\frac{(r - h\xi)^2}{h_0^2 \xi (1 - \xi)} \right] - \exp \left[ -\frac{(r + h\xi)^2}{h_0^2 \xi (1 - \xi)} \right] \right\} \quad (\text{A3.5})$$

This important expression gives the distance probability distribution function of two segments on a Gaussian chain. These segments are located a distance  $\xi L$  (where  $0 < \xi < 1$ ) away from each other, measured along the contour of the chain, while the endpoints of the chain are fixed at a distance  $h$ .

If one assumes that the distribution of a pair of charged segments is neither disturbed by the interactions of these charges themselves nor by the presence of the other charges, the electrostatic free energy can be calculated by adding the average energies of all segment pairs. Realizing that there are  $(q - k)$  distinct pairs of charged segments separated a distance of  $k$  segments along the chain, and postulating Debye-

Table 6. Free Energy of a Lattice Polyelectrolyte of 40 Segments

$q$	$R = 3$	$R = 7$	$R = 11$	$R = 15$	$R = 19$	$R = 23$	$R = 27$	$R = 31$	$R = 35$	$R = 39$
A. Results for $n = 40$ and $\kappa a = 0.0$										
0	-53.3	-53.1	-52.0	-49.9	-46.4	-41.4	-34.7	-25.9	-14.8	0.000
4	-49.1	-49.7	-49.2	-47.6	-44.6	-39.9	-33.3	-24.8	-13.7	0.929
8	-33.3	-34.9	-35.6	-35.3	-33.6	-30.2	-24.8	-17.2	-7.01	6.94
12	-6.49	-9.54	-11.3	-12.3	-12.1	-10.5	-6.86	-0.983	7.64	20.1
16	32.1	27.2	23.8	21.3	19.8	19.6	21.1	24.8	31.2	41.7
20	83.5	75.6	69.3	64.7	61.0	58.6	57.7	59.0	62.8	70.6
24	151	140	130	123	117	111	108	107	108	114
28		214	201	191	181	173	167	163	161	164
32		305	288	273	260	248	237	229	225	226
36		404	387	365	345	328	313	302	294	291
40		517	495	466	443	420	400	383	371	365
B. Results for $n = 40$ and $\kappa a = 0.3$										
0	-53.3	-53.1	-52.0	-49.9	-46.4	-41.4	-34.7	-25.9	-14.8	0.000
4		-52.1	-51.4	-49.5	-46.2	-41.3	-34.6	-25.9	-14.7	0.013
8		-46.9	-46.8	-45.7	-43.2	-39.0	-32.8	-24.5	-13.7	0.743
12		-37.0	-37.6	-37.3	-35.7	-32.4	-27.2	-19.9	-9.94	3.77
16		-22.6	-23.5	-23.9	-23.3	-21.1	-17.1	-11.0	-2.21	10.3
20			-5.59	-6.61	-6.88	-5.84	-3.12	1.57	8.80	19.7
24			21.1	18.9	17.7	17.6	19.1	22.5	28.4	38.2
28			51.5	47.8	45.5	44.2	44.3	46.3	50.9	59.4
32			90.6	84.6	79.7	76.8	75.5	75.9	78.7	85.4
36			133	124	117	112	109	107	108	113
40			178	167	158	151	145	142	140	143
C. Results for $n = 40$ and $\kappa a = 0.6$										
0	-53.3	-53.1	-52.0	-49.9	-46.4	-41.4	-34.7	-25.9	-14.8	0.000
4		-52.7	-51.8	-49.8	-46.4	-41.4	-34.7	-25.9	-14.8	0.000
8		-50.3	-49.8	-48.2	-45.2	-40.6	-34.1	-25.6	-14.5	0.136
12		-45.2	-45.1	-44.0	-41.6	-37.5	-31.6	-23.6	-13.0	1.21
16		-37.2	-37.3	-36.7	-34.9	-31.5	-26.3	-19.0	-9.17	4.31
20			-27.3	-27.1	-25.8	-23.1	-18.7	-12.3	-3.43	9.02
24			-11.4	-11.5	-10.7	-8.64	-4.90	0.774	8.96	20.8
28			6.55	5.92	6.23	7.72	10.7	15.6	23.1	34.3
32			29.1	27.7	27.1	27.8	30.1	34.0	40.4	50.6
36			53.1	50.9	49.3	49.3	50.6	53.5	58.7	67.6
40			78.9	75.5	73.6	72.5	72.4	74.2	77.9	85.3
D. Results for $n = 40$ and $\kappa a = 0.9$										
0	-53.3	-53.1	-52.0	-49.9	-46.4	-41.4	-34.7	-25.9	-14.8	0.000
4		-52.9	-51.9	-49.8	-46.4	-41.4	-34.7	-25.9	-14.8	0.000
8		-51.7	-50.9	-49.1	-45.9	-41.1	-34.5	-25.8	-14.7	0.027
12		-48.7	-48.2	-46.8	-43.9	-39.5	-33.2	-24.9	-14.0	0.434
16		-43.9	-43.6	-42.4	-40.0	-36.0	-30.1	-22.3	-12.0	2.03
20			-37.4	-36.6	-34.5	-31.0	-25.7	-18.4	-8.70	4.56
24			-26.6	-26.0	-24.4	-21.2	-16.3	-9.51	-0.180	12.8
28			-14.6	-14.3	-12.9	-10.2	-5.82	0.566	9.50	22.2
32			0.080	0.174	1.05	3.31	7.17	13.0	21.2	33.2
36			15.6	15.3	15.8	17.6	20.9	25.9	33.4	44.6
40			31.8	31.2	31.5	32.8	35.2	39.5	46.1	56.2

Hückel interactions between all charge pairs, Katchalsky writes

$$F(h, q, \kappa) = \sum_{k=1}^{q-1} (q-k) \int_0^{1/2} Q \frac{\exp(-\kappa r)}{r} W\left(\frac{k}{q}, r, h\right) dr \quad (\text{A3.6})$$

The factor  $1/2$ , introduced by Katchalsky in the expression for the electrostatic energy contribution of a charge pair, which is supposed to be due to charging, is not correct (and therefore is omitted in the course of his calculation without mentioning this), as both charges on the chain have the same sign.  $k/q$  is the contour distance between charges positioned  $k$  segments apart from each other on the chain, relative to the chain length. If the number of charges,  $q$ , is large, the summation can be approximated by an integration,

$$F(h, q, \kappa) = \frac{q^2 Q}{2} \int_0^1 d\xi (1-\xi) \int_0^\infty \frac{\exp(-\kappa r)}{r} W(\xi, r, h) dr \quad (\text{A3.7})$$

For  $\kappa = 0$ , we substitute eq A3.5, and the expression simplifies to

$$F(h, q, 0) = \frac{q^2 Q}{2h} \int_0^1 d\xi \frac{(1-\xi)}{\xi} [\pi h_0^2 \xi (1-\xi)]^{-1/2} \times \int_0^\infty \left\{ \exp\left[-\frac{(r-h\xi)^2}{h_0^2 \xi (1-\xi)}\right] - \exp\left[-\frac{(r+h\xi)^2}{h_0^2 \xi (1-\xi)}\right] \right\} dr \quad (\text{A3.8})$$

The integral over  $r$  can be performed, so that

$$F(h, q, 0) = \frac{q^2 Q}{2h} \int_0^1 d\xi \frac{(1-\xi)}{\xi} \operatorname{erf}\left(\frac{h}{h_0} \sqrt{\frac{\xi}{1-\xi}}\right) \quad (\text{A3.9})$$

Changing to the new variable  $y \equiv (\xi/(1-\xi))^{1/2}$ , and defining  $\alpha = h/h_0$ , we obtain

$$F(h, q, 0) = \frac{q^2 Q}{h} \int_0^\infty dy \frac{1}{y(y^2 + 1)^2} \operatorname{erf}(\alpha y) \quad (\text{A3.10})$$

After differentiating this result with respect to  $\alpha$ , the integral can be performed, and subsequent integration

Table 7. Free Energy of a Lattice Polyelectrolyte of 80 Segments

$q$	$R = 39$	$R = 47$	$R = 55$	$R = 63$	$R = 71$	$R = 79$
A. Results for $n = 80$ and $\kappa a = 0.0$						
0	-98.6	-88.0	-73.8	-55.6	-32.2	0.00
8		-82.4	-69.0	-51.4	-28.5	3.39
16		-55.7	-45.3	-30.4	-9.72	20.2
24			0.956	11.5	28.1	54.3
32			71.7	76.5	87.7	109
40			164	161	166	180
48			288	278	276	285
56			433	414	404	406
64			606	576	555	550
B. Results for $n = 80$ and $\kappa a = 0.3$						
0	-98.6	-88.0	-73.8	-55.6	-32.2	0.000
8	-97.9	-87.6	-73.6	-55.5	-32.1	0.060
16	-91.0	-82.2	-69.3	-52.2	-29.7	1.86
24	-75.1	-68.3	-57.4	-42.2	-21.5	8.48
32	-48.8	-44.2	-36.0	-23.3	-5.03	22.4
40	-14.4	-12.4	-6.95	2.66	17.7	41.9
48	37.7	36.6	39.3	46.2	58.6	80.4
56	97.9	93.0	92.4	96.1	105	124
64	171	161	156	156	162	177
72	250	235	226	221	223	233
80	338	317	302	291	287	293
C. Results for $n = 80$ and $\kappa a = 0.6$						
0	-98.6	-88.0	-73.8	-55.6	-32.2	0.000
8	-98.4	-88.0	-73.8	-55.6	-32.2	0.002
16	-95.7	-86.0	-72.4	-54.7	-31.6	0.363
24	-88.1	-79.5	-67.0	-50.4	-28.3	2.79
32	-74.2	-66.9	-55.9	-40.7	-20.1	9.43
40	-55.6	-49.8	-40.4	-27.1	-8.46	19.0
48	-24.5	-20.0	-12.0	-0.007	17.3	43.7
56	11.0	13.9	20.4	30.7	46.4	71.4
64	53.4	54.7	59.3	67.7	81.3	104
72	99.9	98.9	101	107	118	139
80	150	146	146	149	157	174
D. Results for $n = 80$ and $\kappa a = 0.9$						
0	-98.6	-88.0	-73.8	-55.6	-32.2	0.000
8	-98.5	-88.0	-73.8	-55.6	-32.2	0.000
16	-97.3	-87.1	-73.3	-55.3	-32.1	0.077
24	-93.2	-83.7	-70.6	-53.3	-30.6	1.02
32	-85.1	-76.5	-64.2	-47.8	-26.1	4.48
40	-74.0	-66.3	-55.1	-39.9	-19.6	9.59
48	-53.0	-46.3	-35.9	-21.5	-1.78	26.9
56	-29.5		-14.2	-0.735	18.1	46.0
64	-1.43		11.8	24.1	41.6	68.2
72	29.0		39.5	50.3	66.2	91.2
80	60.4		68.3	77.4	91.4	114

and rearranging yields

$$F(h, q, 0) = \frac{q^2 Q}{h} [\sqrt{\pi} \alpha \exp(\alpha^2) (\operatorname{erf}(\alpha) - 1) + 2\sqrt{\pi} \int_0^\alpha \exp(x^2) (1 - \operatorname{erf}(x)) dx] \quad (\text{A3.11})$$

The latter integral can be approximated using the well-known asymptotic approximation for  $\operatorname{erf}(x)$ , provided  $x$  is large:

$$\operatorname{erf}(x) = 1 - \frac{\exp(-x^2)}{\sqrt{\pi} x} \left( 1 - \frac{1}{2^1 x^2} + \frac{(1)(3)}{2^2 x^4} - \frac{(1)(3)(5)}{2^3 x^6} + \dots \right) \quad (\text{A3.12})$$

Taking only the leading term in this expansion and dropping the factor  $1/2$ , one obtains Katchalsky's result, which is, therefore, only valid for relatively large values of  $h$  (for  $h \geq 4h_0$ , the relative error is smaller than 1%):

$$F(h, q, 0) = \frac{q^2 Q}{h} \left[ 1 + \ln \left( \frac{h^2}{h_0^2} \right) \right] \quad (\text{A3.13})$$

For  $\kappa > 0$ , expression A3.7 seems only a bit more complicated,

$$F(h, q, \kappa) = \frac{q^2 Q}{2h} \int_0^1 d\xi \frac{(1-\xi)}{\xi} [\pi h_0^2 \xi (1-\xi)]^{-1/2} \times \int_0^\infty \left\{ \exp \left[ -\frac{(r-h\xi)^2}{h_0^2 \xi (1-\xi)} - \kappa r \right] - \exp \left[ -\frac{(r+h\xi)^2}{h_0^2 \xi (1-\xi)} - \kappa r \right] \right\} dr \quad (\text{A3.14})$$

but after performing the integration over  $r$ , one obtains

$$F(h, q, \kappa) = \frac{q^2 Q}{4h} \int_0^1 d\xi \frac{1-\xi}{\xi} \exp \left( \frac{\kappa^2 h_0^2 \xi (1-\xi)}{4} \right) \times \left\{ \exp(-\kappa h \xi) \left[ 1 - \operatorname{erf} \left( -\frac{h}{h_0} \sqrt{\frac{\xi}{1-\xi}} + \frac{\kappa h_0 \sqrt{\xi(1-\xi)}}{2} \right) \right] - \exp(\kappa h \xi) \left[ 1 - \operatorname{erf} \left( \frac{h}{h_0} \sqrt{\frac{\xi}{1-\xi}} + \frac{\kappa h_0 \sqrt{\xi(1-\xi)}}{2} \right) \right] \right\} \quad (\text{A3.15})$$

After many simplifications, Katchalsky finds, for "intermediate values of  $\kappa$ ",

$$F(h, q, \kappa) \approx \frac{q^2 Q}{h} \ln \left[ 1 + 4 \frac{h}{\kappa h_0^2} \right] \quad (\text{A3.16})$$

where he again omitted the factor  $1/2$ . To check this result, we approximated expression A3.15 numerically and found that, for  $\kappa h \geq 10$ , the relative error in this approximate result is less than 5% (for  $\kappa h \geq 30$ , the relative error is smaller than 1%). Assuming that  $h^2 > h_0^2 = (2/3)NA^2$ , where  $A$  is the length of a statistical segment and  $N$  the number of segments, we find for the Debye screening parameter the following restriction:  $\kappa A \geq 12/N^{1/2}$ , so, for long chains, eq A3.16 is generally a good approximation for eq A3.15.

However, as mentioned above, in the calculation of the conformational free energy of (highly) charged chains, one should take the influence of the charge interactions on the conformational behavior of the chain into account. This can be done by calculating the electrostatic contribution to the partition sum of the charged polyion, obtained by normalizing the total partition sum by the partition sum of the uncharged chain. The resulting quantity is given by

$$Z(h, q, \kappa) = \int \exp \left\{ - \sum_{i \neq j} \frac{Q_i Q_j}{r_{ij}} \exp(-\kappa r_{ij}) \right\} \times W_t(\{\mathbf{r}_{ij}, n_{ij}\} | h) d\{\mathbf{r}_{ij}\} \quad (\text{A3.17})$$

Here,  $i$  and  $j$  number the segments as in eq 2.9, and the integral is taken over the vectorial distances  $\mathbf{r}_{ij}$  between all possible charge pairs, *i.e.*, for all combinations of  $i$  and  $j$  ( $i \neq j$ ), and thus over all conformations  $\{\mathbf{r}_{ij}\}$ . The exponential factor is the Boltzmann factor, in which the total energy is calculated as a sum of pair interactions between charged segments. Note that the Bjerrum length  $Q$  contains the factor  $1/kT$ , and the factor  $Q_i Q_j$  only counts segment pairs of which both segments are charged. The function  $W_t$  gives the probability of a certain conformation  $\{\mathbf{r}_{ij}\}$ , where  $n_{ij}$  gives the number of segments between segments  $i$  and  $j$  along the chain, the end-to-end distance  $h$  of which is held fixed. As both endpoints are fixed and charged, we can perform the integration over  $\mathbf{r}_{0n}$ , the distance between both endpoints, for which  $W_t$  must be a  $\delta$  function, and we obtain

$$Z(h, q, \kappa) = \exp \left\{ - \frac{Q \exp(-\kappa h)}{h} \right\} \times \left[ \int \exp \left\{ - \sum_{i \neq j} \frac{Q_i Q_j}{r_{ij}} \exp(-\kappa r_{ij}) \right\} W_t(\{\mathbf{r}_{ij}, n_{ij}\} | h) d\{\mathbf{r}_{ij}\} \right] \quad (\text{A3.18})$$

where  $(i, j)$  may not be  $(0, n)$  anymore. It can be shown that, for very small values of the interaction energy (*i.e.*, the summed expression in the exponential tends to zero), this expression reduces to eq A3.6 (except for the erroneous factor of  $1/2$ ), by using eq 2.6 and using first order expansions of  $e^{-x}$  and  $\ln(1 - x)$ .

As there is no expression for the  $W_t$  of a real (*i.e.*, self-avoiding) polymer chain available, we have to make some assumptions. First, we assume that the un-

charged chain behaves in a Gaussian manner, which will be more or less the case if the chain is long and flexible and bare excluded volume effects are relatively small. If we also assume that the contribution due to every pair of charges does not depend strongly on the position of the other charges (this will be the case if the charge density is not too high and the solution contains some added salt), we can write  $W_t$  as a product of pair distributions. As a result, the multiple integral becomes a product of pair integrals, and we may use expression A3.5 for the segment pair distribution function. Clearly, for less than two charges, the argument of the exponential function is zero (there are no charge interactions along the chain). In the case of two charges, these are located at both endpoints. As a result, one obtains eqs 5.4a–c.

The interactions between different charge pairs are assumed to be independent of each other, so that the partition sum can be factorized. Every factor—depending on  $k$ —gives the partition sum of a pair of charges, positioned a distance  $kL/(q - 1)$  along the contour of the chain. As there are  $(q - k)$  of these independent charge pairs, we obtain the exponent  $(q - k)$ , in the same way as the factor  $(q - k)$  emerges in eq A3.6. Note that the integration over the *directions* of every  $\mathbf{r}_{ij}$  is already absorbed in the definition of  $W$ .

Although this expression is much more satisfactory than eq A3.6, still only *pair* interactions are taken into account, and the chain is considered to be *Gaussian*, so the real chain must be sufficiently flexible. For high charge densities and low Debye screening, eq 4.5c will, therefore, certainly not give accurate results. We did not attempt to evaluate the result analytically, as for all values of its parameters the integrand shows a strong peak for relatively small  $r$  values. Therefore, the actual range over which the integration must be performed is small, and the numerical convergence is generally fast.

By taking the natural logarithm of the partition sum (see eq 2.6), the contribution of the charge interactions to the conformational free energy of the chain can be found.

## References and Notes

- (1) Barenbrug, T. M. A. O. M.; Smit, J. A. M.; Bedeaux, D. *Polym. Gels Networks* **1995**, *3*, 331–373.
- (2) Katchalsky, A.; Michaeli, I. *J. Polym. Sci.* **1955**, *15*, 69.
- (3) Katchalsky, A.; Lifson, S.; Eisenberg, H. *J. Polym. Sci.* **1951**, *7*, 571.
- (4) Haša, J.; Ilavský, M.; Dušek, K. *J. Polym. Sci., Polym. Phys. Ed.* **1975**, *13*, 253.
- (5) Tanaka T. *Sci. Am.* **1981**, *244*, 110.
- (6) Ohmine, I.; Tanaka, T. *J. Chem. Phys.* **1982**, *77*, 5725.
- (7) Konac, C.; Bansil, R. *Polymer* **1989**, *30*, 677.
- (8) Barenbrug, T. M. A. O. M.; Smit, J. A. M.; Bedeaux, D. *Macromolecules* **1993**, *26*, 6864. For other chain lengths, one can determine  $R_0^2$  by interpolation using the data for the SC lattice given in the following: Barrett, A. J.; Mansfield, M.; Benesch, B. C. *Macromolecules* **1991**, *24*, 1615. (Note that, for  $N = 416$  their value for  $R_N^2$  is not correct.)
- (9) Le Bret, M.; Zimm, B. H. *Biopolymers* **1984**, *23*, 271.
- (10) Fowler, R.; Guggenheim, E. A. *Statistical Thermodynamics*, 2nd ed.; Cambridge University Press: Cambridge, U.K., 1956; Chapter 9.
- (11) Manning, G. *J. Chem. Phys.* **1969**, *51*, 924.
- (12) Madras, N.; Sokal, A. D. *J. Stat. Phys.* **1990**, *58*, 159.
- (13) Madras, N.; Sokal, A. D. *J. Stat. Phys.* **1988**, *50*, 109.
- (14) Katchalsky, A. *J. Polym. Sci.* **1952**, *7*, 393.
- (15) Katchalsky, A. *J. Polym. Sci.* **1955**, *15*, 69.
- (16) Bishop, M.; Clarke, J. H. R. *J. Chem. Phys.* **1991**, *94*, 3936. Eisenberg, N.; Klafter, J. *J. Chem. Phys.* **1993**, *99*, 3976.